Published in final edited form as:
Ultrasonics. 2012 September ; 52(7): 803–808. doi:10.1016/j.ultras.2012.03.002.

Fluorescence response of human HER2+ cancer- and MCF-12F normal cells to 200 MHz ultrasound microbeam stimulation: a preliminary study of membrane permeability variation

Jae Youn Hwang[1,*], **Jungwoo Lee**[2,*,+], **Changyang Lee**[3], **Anette Jakob**[4], **Robert Lemor**[4], **Lali K. Medina-Kauwe**[1,5], and **K. Kirk Shung**[3]

[1]Department of Biomedical Sciences, Cedars-Sinai Medical Center, Los Angeles, CA 90048, USA

[2]Department of Electronic Engineering, Kwangwoon University, Seoul, Republic of Korea, 137-701

[3]Department of Biomedical Engineering, University of Southern California, Los Angeles, CA 90089, USA

[4]Fraunhofer IBMT for Biomedical Engineering, Division Ultrasound, St. Ingbert, Germany

[5]Department of Medicine, University of California Los Angeles, Geffen School of Medicine, Los Angeles, CA 90048, USA

Abstract

Targeted mechanical cell stimulation has been extensively studied for a better understanding of its effect on cellular mechanotransduction signaling pathways and structures by utilizing a variety of mechanical sources. In this work, an ultrasound-driven single cell stimulation method is thus proposed, and a preliminary study is carried out by comparing the fluorescence intensities representing a change in cell membrane permeability between MDA-MB-435 human HER2+ cancer cells (~40-50 μm in diameter) and MCF-12F normal cells (~50-60 μm) in the presence of ultrasound. A 200 MHz single element zinc oxide (ZnO) transducer is employed to generate ultrasound microbeam (UM) whose beamwidth and depth of focus are 9.5 μm and 60 μm, comparable to typical cell size. The cells in tetramethyl rhodamine methyl ester (TMRM) are interrogated with 200 MHz sinusoidal bursts. The number of cycles per burst is 5 and the pulse repetition frequency (*PRF*) is 1 kHz. The temporal variation of fluorescence intensity in each cell is measured as a function of input voltage to the transducer (16, 32, and 47 V), and its corresponding fluorescence images are obtained via a confocal microscope. A systematic method for visualizing UM's focus by adding Rhodamine B to the immersion medium is also proposed to enhance the precision in aiming the beam at an individual cell.

Both types of cells exhibit a decrease in the intensity upon UM irradiation. In particular, normal cells show more fluorescence reduction (down to 0.7 in normalized intensity) than cancer cells (~ 0.9) under the same excitation condition of the transducer. With UM being turned off, the

[+]**Corresponding author: Jungwoo Lee** Address: Wolgye 447-1, Nowon, Seoul, Republic of Korea, 139-701 Tel: (+82) 02-940-5393 Fax: (+82) 02-942-5235 jwlee@kw.ac.kr.
[*]Equal contribution

normalized intensity level in normal cells is slowly increased to 1.1. The cell images taken before and after UM exposure indicate that the intensity reduction is more pronounced in those cells after exposure. Hence the results show the potential of UM as a non-invasive in vitro stimulation tool for facilitating targeted drug delivery and gene transfection as well as for studying cellular mechanotransduction.

Keywords

Ultrasound microbeam; Mechanotransduction; Mechanical stimulation; Fluorescence intensity; membrane permeability

Introduction

Dynamic cellular responses to externally applied forces that induce various aspects of cell behaviors [1] have long been of scientific interest to many researchers. Such an emerging interest has led to the development of a number of approaches in applying external forces to cells and tissue cultures for mechanotransduction studies [2]. In particular, electric stimulation of ganglion cells using multi-electrodes has offered a better understanding of how to activate neurons with extracellular electric stimuli applied to the retinal surface. Stimulation current varying from 0.6 to 16.7 μA has been applied to the retinal tissue (1-2 mm in diameter) separated from the pigment epithelium [3]. The effect of in vitro electrical stimulation on generation of reactive oxygen species and cardiogenesis in embryoid bodies derived from human embryonic stem cells has been investigated in a custom-built electrical bioreactor under the electrical field of 1 V/mm [4]. Transcranial magnetic stimulation has also been carried out to study its influence on electroencephalography (EEG) oscillatory activity in motor cortex of healthy human brain [5]. In order to reveal the relation between magnetic field and cortical excitability modulation, a maximum field of 2.2 Tesla produced from a commercial magnetic stimulator (Magstim Company, Whitland, UK) has been applied to the primary cortex at 1 Hz for 10 minutes.

In contrast to complex experimental systems and high implementation cost of the aforementioned approaches, ultrasound can be an alternative stimulation tool, because it is simple and inexpensive to construct such systems. Low intensity (up to 400 mW/cm^2) ultrasound stimulation has been demonstrated to induce chondrogenic differentiation of mesenchymal stem cells *in vitro* for cartilage tissue engineering [6], whereas techniques for ultrasound-enhanced drug delivery has been developed with high intensity ultrasound (~ 2660 W/cm^2) [7]. Temporary pore formation in the membrane caused by ultrasonic irradiation has also been utilized to improve nanoparticle penetration into breast cancer spheroids [8] and chemotherapeutic efficacy in retinoblastoma cells *in vitro* [9]. In these low frequency (1-2 MHz) techniques, however, multiple cells have been simultaneously exposed to sound beams with the beamwidth of several hundred micrometers.

In order to promote individual cellular interaction with ultrasound, a narrow beamwidth approaching a certain cell size is crucial. This can be made possible as the frequency is increased to beyond 100 MHz at which the beamwidth may become as narrow as a few μm. Ultrasound of 100 MHz to a few GHz range is here termed as ultrasound microbeam (UM). As an application of UM, two-dimensional cell manipulation has been experimentally demonstrated with 200 MHz sinusoidal bursts (*PRF* = 1 kHz, duty factor = 0.025 %, and supplied voltage to the transducer = 2 V), showing that the beam is capable of trapping a leukemia cell at the focus without affecting other neighboring cells [10]. Elastic properties of zebrafish embryos are parametrically mapped through acoustic radiation force impulse imaging at 100 MHz [11].

More recently, it has been found that tetramethyl rhodamine methyl ester (TMRM) fluorescence accumulated in mitochondria can be used as an indicator of mitochondrial membrane permeability [12]. Therefore it can readily be envisioned that the change in the cell membrane permeability resulted from targeted UM irradiation may be monitored by measuring the fluorescence intensity arising from an individual cell.

In this paper, a preliminary study to demonstrate the feasibility for the use of UM as a targeted mechanical cell stimulation tool is undertaken by measuring the fluorescence modulation of cancer (MDA-MB-435) and normal cells (MCF-12F) in the presence of TMRM. Those cells are non-invasively stimulated by a focused ZnO transducer at 200 MHz. The effect of UM interrogation on each cell is evaluated with respect to the fluorescence intensity by a confocal microscope. The temporal intensity changes of TMRM are compared between the cell groups, as a function of ultrasonic beam intensity represented by the supplied voltage to the transducer here, given that there exists no device that is capable of measuring ultrasonic intensity at such high frequencies (> 100 MHz). A systematic approach for defining UM's focus is also devised by adding heat-sensitive Rhodamine B to the immersion medium, allowing more accurate exposure of a single cell to UM. The results are reported to show the UM's capability as an alternative means for targeted drug delivery and cellular mechanotransduction study.

Materials and Methods

Cell preparation

MDA-MB-435 human HER2+ cancer cell (~40-50 μm in diameter) and MCF-12F normal cell (~50-60 μm) lines are obtained from the National Cancer Institute and ATCC (American Type Culture Collection), and maintained in DMEM, 10 % fetal bovine serum under 5 % CO_2. TMRM is purchased from Invitrogen (Grand Island, NY) and laser grade rhodamine B is obtained from Acros Organics (Pittsburgh, PA). Carbonate buffer, 20 mM/L at pH 9.4, is also prepared to make Rhodamine B solutions (0.1 mM/L). Temperature around the cells is maintained at 37 °C in a delta T chamber controlled by a thermal instrument (Bioptechs, USA). The bottom of the chamber is made of an acoustically transparent polyimide film (Kapton Type HN, DuPont, USA) for minimizing a strong reflection from the below at the cell-chamber interface otherwise. Please note that the reflection coefficient is 0.94 at a water-stainless steel interface [13].

UM stimulation and confocal imaging systems

Fig. 1 illustrates the system layout including two sub-systems for UM stimulation and confocal fluorescence imaging. Conventional transducer fabrication procedure for acoustic microscopy [14] has been utilized to construct a single element ZnO transducer for 200 MHz UM generation. A 6 μm thick ZnO plate is sputtered between two gold electrode layers on the back side of a sapphire (Al_2O_3) buffer rod. UM arising from the ZnO plate is transmitted to a spherical cavity at the tip of the rod that works as a focusing lens. A quarter-wavelength glass layer is added to the front side of the cavity as an acoustic matching between the lens and the cell suspension.

The transducer's focal length is 546 μm and its aperture diameter is 570 μm. The transducer's bandwidth is 30 % (Fig. 2a). It is practically impossible at present to determine the transmitted sound pressures from the transducer, because there are no established methods for calibrating absolute pressure level in UM's frequency range. The lateral beam profile is thus obtained by scanning a tungsten wire target that has a 3 μm diameter. The measured beamwidth is found to be 9.5 μm (Fig. 2b), close to the predicted value of 7.5 μm (= focal length × wavelength / aperture diameter) and the actual depth of focus is 60 μm

(Fig. 2c). The excitation signal for the transducer is shown in Fig. 2d. 200 MHz sinusoidal bursts are supplied from a function generator (AFG 3251, Tektronix, USA) to the transducer, followed by a 50-dB power amplifier (525LA, ENI, USA). The resultant peak-to-peak (V_{pp}) voltage of the burst with the transducer being loaded is adjusted to 16, 32, and 47 V. The number of cycles is 5 per burst, and the *PRF* is 1 kHz.

Fluorescence live cell imaging is carried out to monitor the cellular response to UM stimuli with a Leica TCS SPE confocal microscope. Laser light chosen by an acousto-optical tunable filter (AOTF) is delivered to those cells for excitation (ex) after passing through an excitation pinhole, galvo-mirrors, a dichroic mirror, and a 40 × objective. The light emitted from the cells is then collected by the same objective and recorded in a photomultiplier tube (PMT) detector via an emission pinhole and AOTF, which allows the selection of proper emission (em) wavelengths.

Visualization of UM focus

For targeted cell stimulation, it is extremely important to accurately find the position of the UM's focal spot in the field of view (FOV) of interest, to ensure that 9.5 μm beamwidth is centered on individual cells whose mean diameter varies between 40 μm and 60 μm in this case. Temperature changes are probed to visually locate the UM's focus with Rhodamine B [15], a temperature-sensitive fluorophore. The transducer's position is controlled by a three-axis manual linear stage (OptoSigma, USA). The center of the transducer is first placed at the center of the FOV through bright-field imaging. Pulse echo tests are then conducted to axially fix the transducer at the UM's focal distance, the bottom surface of a delta T chamber. After a pulser (Model 5900PR, Panametrics, USA) with 200 MHz bandwidth drives the transducer only to transmit a 5 nsec pulse to a flat quartz reflector, an echo is received through a digital oscilloscope (Waverunner 104MXi, LeCroy, USA) whose bandwidth is 1 GHz. When the echo is found at t = 728 nsec, the axial focal length is equal to 546 μm. After the fluorophore solution is added into the chamber, fluorescence images (ex: 535 nm, em: 580 nm) are sequentially acquired before- and after UM applications. While fluorescence images are acquired every 1 sec for t = 600 sec, UM is switched on at t = 100 sec, and then turned off at t = 500 sec.

Rhodamine B fluorescence images are compared before- and after UM exposure, as depicted in Fig. 3. With the transducer's surface shown (Fig. 3a), no fluorescence change is detected before the beam interrogation, while the fluorescence intensity is increased only at the center of the FOV where the focus of UM is positioned (Fig. 3b).

TMRM live cell imaging

TMRM have been widely used as cationic dye for measuring mitochondrial membrane potentials that indicate the variation of membrane permeability. Nernst equation [16] has been frequently employed in physiology to determine the membrane potential with respect to various parameters such as ion concentration existing in membrane/cytoplasm, temperature, and ion charge. According to Nernst equation, an increase in intracellular fluorescence intensity is caused by TMRM's cationic accumulation in intact mitochondria, whereas TMRM diffusion into cytoplasm reduces the intensity. To make sure of precise measurement of TMRM fluorescence, all the images are taken after TMRM level in mitochondria reaches the equilibrium state (~1 h) [17]. The cells are plated at 10^4 cells in each chamber and incubated at 37°C for 36 hours, before 30 nM TMRM is added into the chamber. The number of the cells is counted with a hemocytometer prior to placing them into the chamber. After the location of UM exposure is visually confirmed, the cells are placed at the focus and then a time-lapse confocal imaging is initiated. Laser light at 537 nm is employed to excite the cells, and the emission light within 550 - 590 nm is selected with

an AOTF for TMRM detection. Fluorescence images are acquired every one minute for t = 30 min, as UM is switched on and off at t = 5 min and t = 15 min, respectively.

Results and Discussion

The fluorescence intensity is normalized by the mean intensity for 150 sec before UM onset. The time duration of 150 sec is selected to make sure that all the fluctuation of fluorescence intensity before UM application reaches the equilibrium state. The normalized intensity in targeted cells is plotted over time along with the corresponding TMRM images. In Fig. 4a, both cancer and normal cells exposed to UM exhibit a decrease in the intensity, whereas little intensity change is shown in the control state (when the cells are not near the focus). Particularly, normal cells bear more fluorescence decrease (down to 0.7 in normalized intensity) than cancer cells (~ 0.9) during UM onset. The cellular images taken before- and after UM emission demonstrate that the reduction in intensity is more pronounced in those cells after stimulation (Fig. 4b). When UM is tuned off, in contrast, the intensity level of normal cells are slowly increased to 1.1 with random fluctuation.

Fig. 5 depicts the fluorescence intensity variation as a function of input V_{pp} to the transducer. The intensity is more decreased as higher input voltage is applied. Furthermore, normal cells exhibit more significant decrease in TMRM fluorescence than cancer cells at each voltage. Statistical comparisons are made via a Student's t-test of equal variance with a significance limit of $P < 0.01$. Here, P is found in the range of 10^{-10}, 1.17×10^{-10} at 47 V for example. The mean and standard deviation of the normalized intensity corresponding to variable input voltage are calculated for both cell types to evaluate the effect of microbeam exposure level on the fluorescence response of each cell group, as summarized in Table 1. The number of cells used for statistical analysis is 15 in each voltage condition. Such reduction may be attributed to increased mitochondrial membrane permeability due to the following factors. 1) Ca^{2+} accumulation in mitochondrial matrix causes mitochondrial pores to open as voltage-operated channels, increasing mitochondrial membrane permeability [18, 19]. 2) Cytosolic Ca^{2+} transient can also modulate a potential difference across inner mitochondrial membrane. The concentration change of Ca^{2+} in mitochondria or cytoplasm can be monitored by measuring the fluorescence intensity of intracellular calcium indicators via fluorescence live cell imaging. In contrast, the mitochondrial membrane potential can be measured with the fluorescence intensity of Rhodamine-derivative cationic dyes distributed over those regions [20, 21]. 3) Free radicals e.g., reactive oxygen species (ROS) are generated in cytoplasm, depending on excessive intracellular Ca^{2+} concentration and external mechanical stress [22]. Superoxide, hydrogen peroxide, and hydroxyl radicals are typically associated with mitochondrial damage that breaks up its membrane and leads to permeability increase. The quantitative measurement of ROS can be undertaken by using live cell imaging of ROS detection probes [23]. 4) Mitochondria morphology change or mitochondria rearrangement upon UM application can affect the fluorescence decrease. [24] The effect of such structural change on the fluorescence can be evaluated by using three-dimensional confocal fluorescence imaging of Mitotracker (Invitrogen, USA) or Rhodamine-derivative cationic dyes accumulated in mitochondria [25].

The results demonstrate that cellular responses to UM stimuli may be dependent on the state of a cell. Because the fluorescence expression is proportional to the amount of TMRM absorbed through the membrane, this UM approach may also be developed to efficiently deliver drugs, genes, or protein to particular cells by inducing the membrane permeability variation with targeted beams in addition to studying cellular mechanotransduction mechanisms.

Conclusion

This paper presents preliminary results to demonstrate the potential use of UM as targeted mechanical cell stimulation. Cancer and normal cells are non-invasively stimulated by UM at 200 MHz emitted from a single element ZnO transducer. TMRM fluorescence response of each cell to UM irradiation is quantitatively evaluated on the focal plane by measuring the fluorescence intensity via a confocal microscope. A systematic approach for precisely positioning the UM exposure to designated cells is also developed by visually locating the UM's focus with Rhodamine B. The intensity modulation is compared between different types of cells with respect to the supplied voltage to the transducer. At a given voltage, the fluorescence intensity for normal cells is more decreased than for cancer cells, and more intensity reduction occurs in both cell types after UM irradiation. These results thus indicate that such distinct pattern may depend on the cell type and the exposure condition.

Due to the complicated nature of in vivo experiments, these preliminary results are reported with the ultimate goal of developing this ultrasonic technique as an in vitro laboratory apparatus that can individually provide biological cells with controlled mechanical stimulation. By affecting little influence on neighboring cells, such mechanical disturbance can be applied to each cell both precisely and homogeneously. Hence this proposed method may be useful for examining the relation of external ultrasonic stimulus to in vitro cellular behavior, and for developing in vitro low-dose drug delivery approaches by modulating the membrane permeability with targeted mechanical disturbance.

Acknowledgments

This work has been supported by the NIH grants (R01-EB012058, and P41-EB2182 to K.K. Shung; R21-CA116014, R01-CA140995, and R01-CA129822 to Lali K. Medina-Kauwe). The present research has been conducted by the Research Grant of Kwangwoon University in 2011.

References

1. Hoffman BD, Crocker JC. Cell mechanics: dissecting the physical responses of cells to force. Annu. Rev. Biomed. Eng. 2009; 11:259–288. [PubMed: 19400709]
2. Brown TD. Techniques for mechanical stimulation of cells in vitro: a review. J. Biomech. 2000; 33:3–14. [PubMed: 10609513]
3. Sekirnjak C, Hottowy P, Sher A, Dabrowski W, Litke AM, Chichilnisky EJ. Electrical stimulation of mammalian retinal ganglion cells with multielectrode arrays. J. Neurophysiol. 2006; 95:3311–3327. [PubMed: 16436479]
4. Serena E, Figallo E, Tandon N, Cannizzaro C, Gerecht S, Elvassore N, Vunjak-Novakovic G. Electrical stimulation of human embryonic stem cells: cardiac differentiation and the generation of reactive oxygen species. Exp. Cell. Res. 2009; 315:3611–3619. [PubMed: 19720058]
5. Brignani D, Manganotti P, Rossini PM, Miniussi C. Modulation of cortical oscillatory activity during transcranial magnetic stimulation. Human Brain Mapping. 2008; 29:603–612. [PubMed: 17557296]
6. Lee HJ, Choi BH, Min BH, Son YS, Park SR. Low-intensity ultrasound stimulation enhances chondrogenic differentiation in alginate culture of mesenchymal stem cells. Artif. Organs. 2006; 30:707–715. [PubMed: 16934100]
7. Hancock HA, Smith LH, Cuesta J, Durrani AK, Angstadt M, Palmeri ML, Kimmel E, Frenkel V. Investigations into pulsed high intensity focused ultrasound enhanced delivery: preliminary evidence for a novel mechanism. Ultrasound Med. Biol. 2009; 35:1722–1736. [PubMed: 19616368]
8. Grainger SJ, Serna JV, Sunny S, Zhou Y, Deng CX, El-sayed ME. Pulsed ultrasound enhances nanoparticle penetration into breast cancer spheroids. Mol. Pharm. 2010; 7:2006–2019. [PubMed: 20957996]

9. Lee NG, Berry JL, Lee TC, Wang AT, Honowitz S, Murphree AL, Varshney N, Hinton DR, Fawzi AA. Sonoporation enhances chemotherapeutic efficacy in retinoblastoma cells in vitro. Invest. Ophthalmol. Vis. Sci. 2011; 52:3868–3873. [PubMed: 21273549]
10. Lee J, Lee C, Kim HH, Jakob A, Lemor R, Shung KK. Targeted cell immobilization by ultrasound microbeam. Biotechnol. Bioeng. 2011; 108:1643–1650. [PubMed: 21328319]
11. Park J, Lee J, Lau ST, Lee C, Huang Y, Lien C-L, Shung KK. Acoustic Radiation Force Impulse (ARFI) Imaging of Zebrafish Embryo by High-Frequency Coded Excitation Sequence. Ann. Biomed. Eng. 2012; X:XXX–XXX. (Online First™, in press).
12. Beatrice MC, Palmer JW, Pfeiffe DR. The Relationship between Mitochondrial Membrane Permeability, Membrane Potential, and the Retention of Ca^{2+} by Mitochondria*. J. Biol. Chem. 1980; 25:8663–8671. [PubMed: 7410387]
13. Hall TJ, Madsen EL, Dong F, Medina IR, Frank GR. Low reflection coefficient liquid interfaces for system characterization. Ultrasound Med. Biol. 2001; 27:1003–1010. [PubMed: 11476935]
14. Atalar A, Jipson V, Koch R, Quate CF. Acoustic microscopy with microwave frequencies. Ann. Rev. Mater. Sci. 1979; 9:255–281.
15. Ross D, Gaitan M, Locascio LE. Temperature measurement in microfluidic systems using a temperature-dependent fluorescent dye. Anal. Chem. 2001; 73:4117–4123. [PubMed: 11569800]
16. Hwang JY, Lubow J, Sims J, Gray HB, Mahammed A, Gross Z, Farkas DL, Medina-Kauwe LK. Investigating photoexcitation-induced mitochondrial damage by chemotherapeutic corroles using multimode optical imaging. J. Biomed. Opt. 2012; 17:015003–1-11. [PubMed: 22352647]
17. Hwang JY, Lubow J, Chu D, Ma J, Agadjanian H, Sims J, Gray HB, Gross Z, Farkas DL, Medina-Kauwe LK. A mechanistic study of tumor-targeted corrole toxicity. Mol. Pharm. 2011; 8:2233–2243. [PubMed: 21981771]
18. Brustovetsky N, Brustovetsky T, Jemmerson R, Dubinsky JM. Calcium-induced cytochrome c release from CNS mitochondria is associated with the permeability transition and rupture of the outer membrane. J. Neurochem. 2002; 80:207–218. [PubMed: 11902111]
19. Hunter DR, Haworth RA. The Ca^{2+}-induced membrane transition in mitochondria. I. The protective mechanisms. Arch. Biochem. Biophys. 1979; 195:453–459. [PubMed: 383019]
20. Doczi J, Turiak L, Vajda S, Mandi M, Torocsik B, Gerencser AA, Kiss G, Konrad C, Adam-Vizi V, Chinopoulos C. Complex contribution of cyclophilin D to Ca^{2+}-induced permeability transition in brain mitochondria, with relation to the bioenergetic state. J. Biol. Chem. 2011; 286:6345–6353. [PubMed: 21173147]
21. Ahmed SM, Weber JT, Liang S, Willoughby KA, Sitterding HA, Rzigalinski BA, Ellis EF. NMDA receptor activation contributes to a portion of the decreased mitochondrial membrane potential and elevated intracellular free calcium in strain-injured neurons. J. Neurotrauma. 2002; 19:1619–1629. [PubMed: 12542862]
22. Brustovetsky N, Brustovetsky T, Purl KJ, Capano M, Crompton M, Dubinsky JM. Increased susceptibility of striatal mitochondria to calcium-induced permeability transition. J. Neurosci. 2003; 23:4858–4867. [PubMed: 12832508]
23. Zhou R, Yazdi AS, Menu P, Tschopp J. A role for mitochondria in NLRP3 inflammasome activation. Nature. 2011; 469:221–225. [PubMed: 21124315]
24. Neutzner A, Youle RJ. Instability of the mitofusin Fzo1 regulates mitochondrial morphology during the mating response of the yeast Saccharomyces cerevisiae. J. Biol. Chem. 2005; 280:18598–18603. [PubMed: 15760898]
25. Buckman JF, Hernández H, Kress GJ, Votyakova TV, Pal S, Reynolds IJ. MitoTracker labeling in primary neuronal and astrocytic cultures: influence of mitochondrial membrane potential and oxidants. J. Neurosci. Methods. 2001; 104:165–176. [PubMed: 11164242]

- Investigation into the use of ultrasound microbeam as a mechanical stimulation tool.
- Fluorescence change in cancer- and normal cells under 200 MHz ultrasound.
- More reduction of fluorescence intensity in normal cells than in cancer cells.
- More intensity reduction after UM exposure in both types of cells.
- Systematic visualization of the beam's focus with heat-sensitive fluorescence dye.

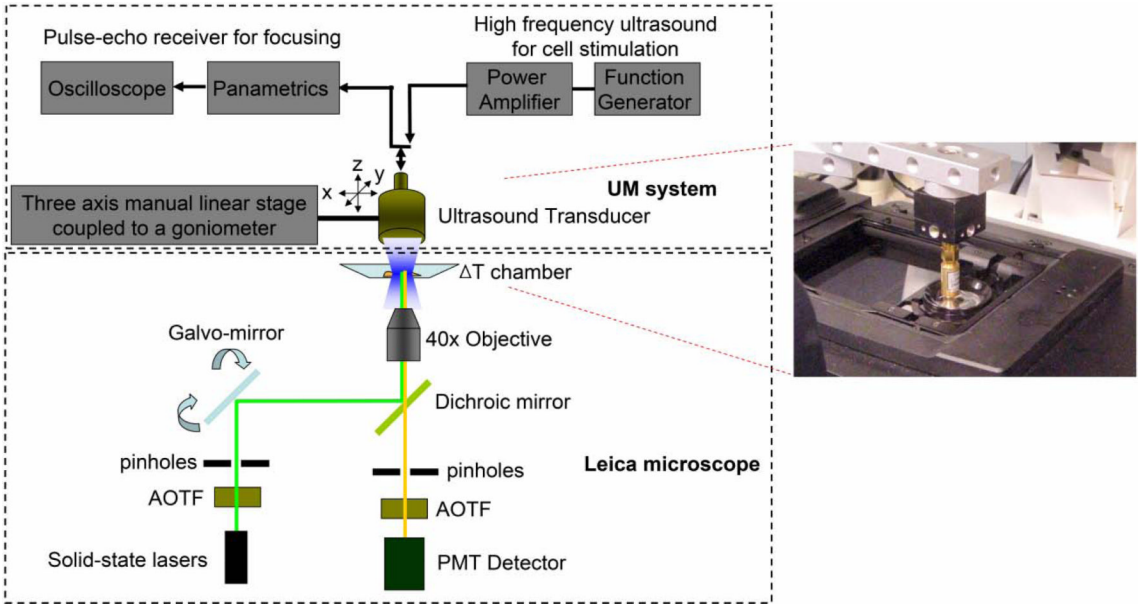

Fig. 1.

Ultrasound microbeam mechanotransduction system. The system is comprised of a 200 MHz ultrasonic transducer for microbeam emission (inset) and a confocal microscope for fluorescence detection.

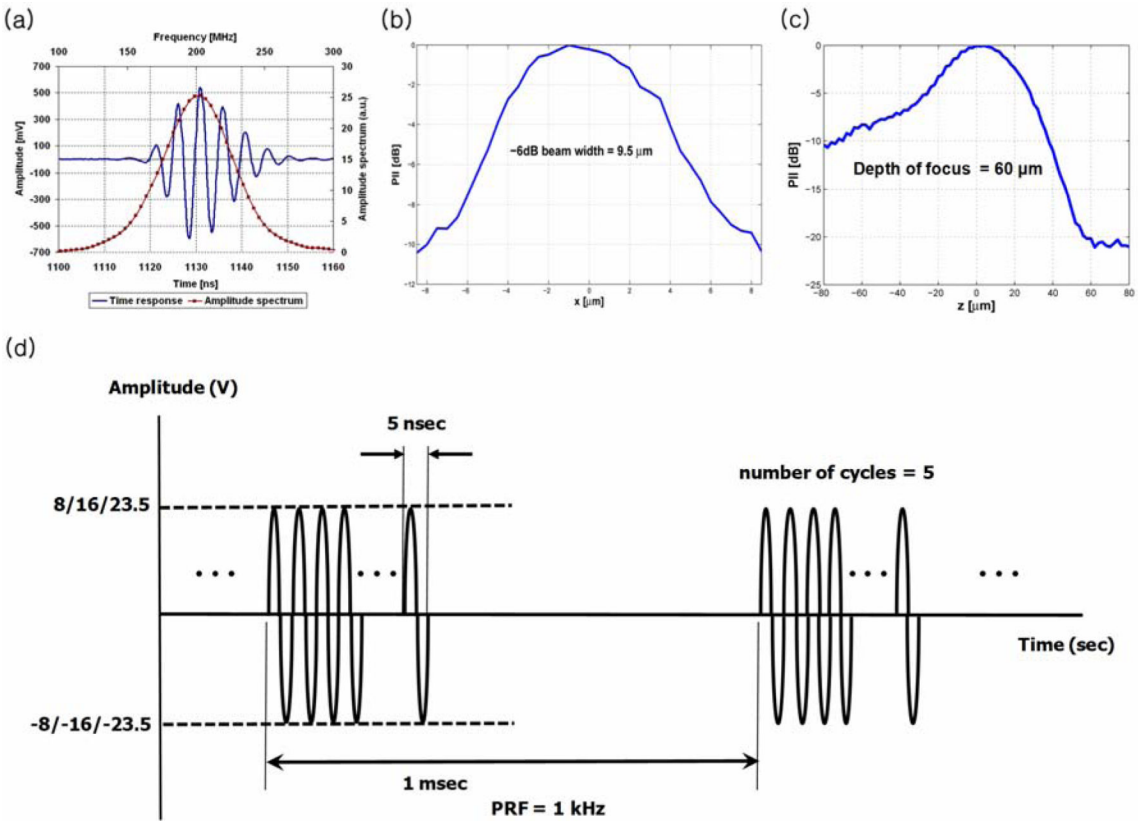

Fig. 2.

Pulse echo response and beam profile of 200 MHz zinc oxide transducer provided by the Fraunhofer Institute for Biomedical Engineering (adopted from [11]) along with the schematic diagram of excitation signal for the transducer. (a) A received echo waveform (solid line) and its frequency spectrum (solid-dotted line) are displayed. (b) The measured beamwidth is 9.5 μm, and (c) the depth of focus is 60 μm in the axial direction. (d) Supplied peak-to-peak voltages to the transducer are 16, 32, 47 V, respectively. Each burst has a duration of 25 nsec, repeated every 1 msec.

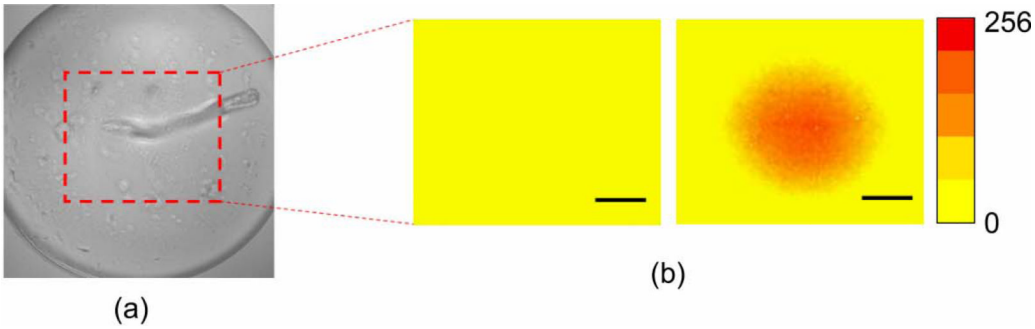

Fig. 3.
Visualization of beam's focus using Rhodamine B dye: (a) Surface of the transducer. (b) Fluorescence images taken before (left) and after (right) ultrasound application (scale bar = 50 μm).

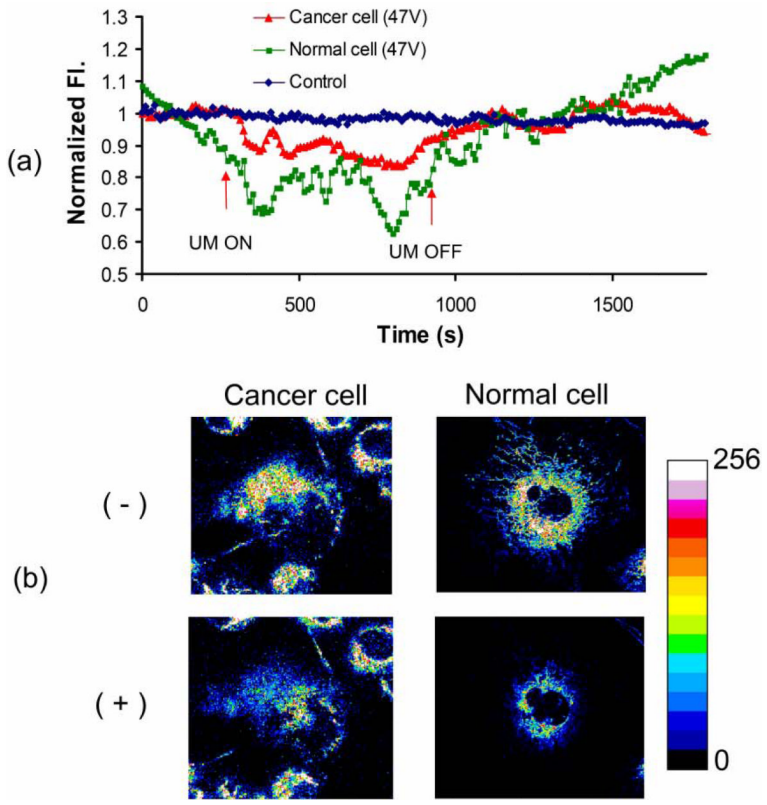

Fig. 4.

TMRM (tetramethyl rhodamine methyl ester) intensity change in cancer and normal cells. (a) The fluorescence change is monitored over time. The arrow indicates the point when ultrasound is turned on or off. (b) Images of cancer and normal cells are obtained before (-) and after (+) microbeam stimulus.

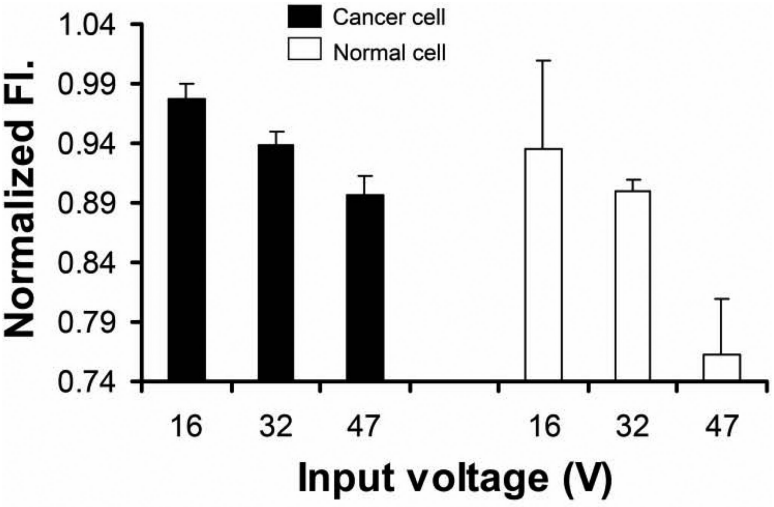

Fig. 5.
Voltage dependence of TMRM (tetramethyl rhodamine methyl ester) fluorescence intensity in different types of cells.

Table 1

Mean and standard deviation of normalized fluorescence intensity response to variable input voltage to the transducer in MDA-MB-435 (cancer cells) and MCF-12F (normal cells). The number of cells used for statistics is 15 in each condition.

	MDA-MB-435 (cancer cells)			**MCF-12F(normal cells)**		
Input voltage (V)	16	32	47	16	32	47
Mean	0.978	0.939	0.896	0.934	0.899	0.763
Standard deviation	0.012	0.010	0.016	0.075	0.011	0.047